

Observation of Seven Astrophysical Tau Neutrino Candidates with IceCube

R. Abbasi,¹⁷ M. Ackermann,⁶² J. Adams,¹⁸ S. K. Agarwalla,^{40,*} J. A. Aguilar,¹² M. Ahlers,²² J. M. Alameddine,²³ N. M. Amin,⁴⁴ K. Andeen,⁴² G. Anton,²⁶ C. Argüelles,¹⁴ Y. Ashida,⁵³ S. Athanasiadou,⁶² S. N. Axani,⁴⁴ X. Bai,⁵⁰ V. A. Balagopal,⁴⁰ M. Baricevic,⁴⁰ S. W. Barwick,³⁰ V. Basu,⁴⁰ R. Bay,⁸ J. J. Beatty,^{20,21} J. Becker Tjus,^{11,†} J. Beise,⁶⁰ C. Bellenghi,²⁷ C. Benning,¹ S. BenZvi,⁵² D. Berley,¹⁹ E. Bernardini,⁴⁸ D. Z. Besson,³⁶ E. Blaufuss,¹⁹ S. Blot,⁶² F. Bontempo,³¹ J. Y. Book,¹⁴ C. Boscolo Meneguolo,⁴⁸ S. Böser,⁴¹ O. Botner,⁶⁰ J. Böttcher,¹ E. Bourbeau,²² J. Braun,⁴⁰ B. Brinson,⁶ J. Brostean-Kaiser,⁶² R. T. Burley,² R. S. Busse,⁴³ D. Butterfield,⁴⁰ M. A. Campana,⁴⁹ K. Carloni,¹⁴ E. G. Carnie-Bronca,² S. Chattopadhyay,^{40,*} N. Chau,¹² C. Chen,⁶ Z. Chen,⁵⁵ D. Chirkin,⁴⁰ S. Choi,⁵⁶ B. A. Clark,¹⁹ L. Classen,⁴³ A. Coleman,⁶⁰ G. H. Collin,¹⁵ A. Connolly,^{20,21} J. M. Conrad,¹⁵ P. Coppin,¹³ P. Correa,¹³ D. F. Cowen,^{58,59} P. Dave,⁶ C. De Clercq,¹³ J. J. DeLaunay,⁵⁷ D. Delgado,¹⁴ S. Deng,¹ K. Deoskar,⁵⁴ A. Desai,⁴⁰ P. Desiati,⁴⁰ K. D. de Vries,¹³ G. de Wasseige,³⁷ T. DeYoung,²⁴ A. Diaz,¹⁵ J. C. Díaz-Vélez,⁴⁰ M. Dittmer,⁴³ A. Domi,²⁶ H. Dujmovic,⁴⁰ M. A. DuVernois,⁴⁰ T. Ehrhardt,⁴¹ P. Eller,²⁷ E. Ellinger,⁶¹ S. El Mentawi,¹ D. Elsässer,²³ R. Engel,^{31,32} H. Erpenbeck,⁴⁰ J. Evans,¹⁹ P. A. Evenson,⁴⁴ K. L. Fan,¹⁹ K. Fang,⁴⁰ K. Farrag,¹⁶ A. R. Fazely,⁷ N. Feigl,¹⁰ S. Fiedlschuster,²⁶ A. T. Fienberg,⁵⁹ C. Finley,⁵⁴ L. Fischer,⁶² D. Fox,⁵⁸ A. Franckowiak,¹¹ A. Fritz,⁴¹ P. Fürst,¹ J. Gallagher,³⁹ E. Ganster,¹ A. Garcia,¹⁴ L. Gerhardt,⁹ A. Ghadimi,⁵⁷ C. Glaser,⁶⁰ T. Glauch,²⁷ T. Glüsenkamp,^{26,60} N. Goehle,³² J. G. Gonzalez,⁴⁴ S. Goswami,⁵⁷ D. Grant,²⁴ S. J. Gray,¹⁹ O. Gries,¹ S. Griffin,⁴⁰ S. Griswold,⁵² K. M. Groth,²² C. Günther,¹ P. Gutjahr,²³ C. Haack,²⁶ A. Hallgren,⁶⁰ R. Halliday,²⁴ L. Halve,¹ F. Halzen,⁴⁰ H. Hamdaoui,⁵⁵ M. Ha Minh,²⁷ K. Hanson,⁴⁰ J. Hardin,¹⁵ A. A. Harnisch,²⁴ P. Hatch,³³ A. Haungs,³¹ K. Helbing,⁶¹ J. Hellrung,¹¹ F. Henningsen,²⁷ L. Heuermann,¹ N. Heyer,⁶⁰ S. Hickford,⁶¹ A. Hidvegi,⁵⁴ C. Hill,¹⁶ G. C. Hill,² K. D. Hoffman,¹⁹ S. Hori,⁴⁰ K. Hoshina,^{40,‡} W. Hou,³¹ T. Huber,³¹ K. Hultqvist,⁵⁴ M. Hünnefeld,²³ R. Hussain,⁴⁰ K. Hyman,²³ S. In,⁵⁶ A. Ishihara,¹⁶ M. Jacquart,⁴⁰ O. Janik,¹ M. Jansson,⁵⁴ G. S. Japaridze,⁵ M. Jeong,⁵⁶ M. Jin,¹⁴ B. J. P. Jones,⁴ D. Kang,³¹ W. Kang,⁵⁶ X. Kang,⁴⁹ A. Kappes,⁴³ D. Kappesser,⁴¹ L. Kardum,²³ T. Karg,⁶² M. Karl,²⁷ A. Karle,⁴⁰ U. Katz,²⁶ M. Kauer,⁴⁰ J. L. Kelley,⁴⁰ A. Khatee Zathul,⁴⁰ A. Kheirandish,^{34,35} J. Kiryluk,⁵⁵ S. R. Klein,^{8,9} A. Kochocki,²⁴ R. Koirala,⁴⁴ H. Kolanoski,¹⁰ T. Kontrimas,²⁷ L. Köpke,⁴¹ C. Kopper,²⁶ D. J. Koskinen,²² P. Koundal,³¹ M. Kovacevich,⁴⁹ M. Kowalski,^{10,62} T. Kozynets,²² J. Krishnamoorthi,^{40,*} K. Kruiswijk,³⁷ E. Krupczak,²⁴ A. Kumar,⁶² E. Kun,¹¹ N. Kurahashi,⁴⁹ N. Lad,⁶² C. Lagunas Gualda,⁶² M. Lamoureux,³⁷ M. J. Larson,¹⁹ S. Latseva,¹ F. Lauber,⁶¹ J. P. Lazar,^{14,40} J. W. Lee,⁵⁶ K. Leonard DeHolton,⁵⁹ A. Leszczyńska,⁴⁴ M. Lincetto,¹¹ Q. R. Liu,⁴⁰ M. Liubarska,²⁵ E. Lohfink,⁴¹ C. Love,⁴⁹ C. J. Lozano Mariscal,⁴³ F. Lucarelli,²⁸ W. Luszczyk,^{20,21} Y. Lyu,^{8,9} J. Madsen,⁴⁰ K. B. M. Mahn,²⁴ Y. Makino,⁴⁰ E. Manao,²⁷ S. Mancina,^{40,48} W. Marie Sainte,⁴⁰ I. C. Mariş,¹² S. Marka,⁴⁶ Z. Marka,⁴⁶ M. Marsee,⁵⁷ I. Martinez-Soler,¹⁴ R. Maruyama,⁴⁵ F. Mayhew,²⁴ T. McElroy,²⁵ F. McNally,³⁸ J. V. Mead,²² K. Meagher,⁴⁰ S. Mechbal,⁶² A. Medina,²¹ M. Meier,¹⁶ Y. Merckx,¹³ L. Merten,¹¹ J. Micallef,²⁴ J. Mitchell,⁷ T. Montaruli,²⁸ R. W. Moore,²⁵ Y. Morii,¹⁶ R. Morse,⁴⁰ M. Moulai,⁴⁰ T. Mukherjee,³¹ R. Naab,⁶² R. Nagai,¹⁶ M. Nakos,⁴⁰ U. Naumann,⁶¹ J. Necker,⁶² A. Negi,⁴ M. Neumann,⁴³ H. Niederhausen,²⁴ M. U. Nisa,²⁴ A. Noell,¹ A. Novikov,⁴⁴ S. C. Nowicki,²⁴ A. Obertacke Pollmann,¹⁶ V. O'Dell,⁴⁰ M. Oehler,³¹ B. Oeyen,²⁹ A. Olivas,¹⁹ R. Orsoe,²⁷ J. Osborn,⁴⁰ E. O'Sullivan,⁶⁰ H. Pandya,⁴⁴ D. V. Pankova,⁵⁹ N. Park,³³ G. K. Parker,⁴ E. N. Paudel,⁴⁴ L. Paul,^{42,50} C. Pérez de los Heros,⁶⁰ J. Peterson,⁴⁰ S. Philippen,¹ A. Pizzuto,⁴⁰ M. Plum,⁵⁰ A. Pontén,⁶⁰ Y. Popovych,⁴¹ M. Prado Rodriguez,⁴⁰ B. Pries,²⁴ R. Procter-Murphy,¹⁹ G. T. Przybylski,⁹ C. Raab,³⁷ J. Rack-Helleis,⁴¹ K. Rawlins,³ Z. Rechav,⁴⁰ A. Rehman,⁴⁴ P. Reichherzer,¹¹ G. Renzi,¹² E. Resconi,²⁷ S. Reusch,⁶² W. Rhode,²³ B. Riedel,⁴⁰ A. Rifaie,¹ E. J. Roberts,² S. Robertson,^{8,9} S. Rodan,⁵⁶ G. Roellinghoff,⁵⁶ M. Rongen,²⁶ C. Rott,^{53,56} T. Ruhe,²³ L. Ruohan,²⁷ D. Ryckbosch,²⁹ I. Safa,^{14,40} J. Saffer,³² D. Salazar-Gallegos,²⁴ P. Sampathkumar,³¹ S. E. Sanchez Herrera,²⁴ A. Sandrock,⁶¹ M. Santander,⁵⁷ S. Sarkar,²⁵ S. Sarkar,⁴⁷ J. Savelberg,¹ P. Savina,⁴⁰ M. Schaufel,¹ H. Schieler,³¹ S. Schindler,²⁶ L. Schlickmann,¹ B. Schlüter,⁴³ F. Schlüter,¹² N. Schmeisser,⁶¹ T. Schmidt,¹⁹ J. Schneider,²⁶ F. G. Schröder,^{31,44} L. Schumacher,²⁶ G. Schwefer,¹ S. Sclafani,¹⁹ D. Seckel,⁴⁴ M. Seikh,³⁶ S. Seunarine,⁵¹ R. Shah,⁴⁹ A. Sharma,⁶⁰ S. Shefali,³² N. Shimizu,¹⁶ M. Silva,⁴⁰ B. Skrzypek,¹⁴ B. Smithers,⁴ R. Snihur,⁴⁰ J. Soedingrekso,²³ A. Sjøgaard,²² D. Soldin,³² P. Soldin,¹ G. Sommani,¹¹ C. Spannfellner,²⁷ G. M. Spiczak,⁵¹ M. Stamatikos,²¹ T. Stanev,⁴⁴ T. Stezelberger,⁹ T. Stürwald,⁶¹ T. Stuttard,²² G. W. Sullivan,¹⁹ I. Taboada,⁶ S. Ter-Antonyan,⁷ M. Thiesmeyer,¹ W. G. Thompson,¹⁴ J. Thwaites,⁴⁰ S. Tilav,⁴⁴ K. Tollefson,²⁴ C. Tönnis,⁵⁶ S. Toscano,¹² D. Tosi,⁴⁰ A. Trettin,⁶² C. F. Tung,⁶ R. Turcotte,³¹ J. P. Twagirayezu,²⁴ B. Ty,⁴⁰ M. A. Unland Elorrieta,⁴³ A. K. Upadhyay,^{40,*} K. Upshaw,⁷ N. Valtonen-Mattila,⁶⁰ J. Vandenbroucke,⁴⁰ N. van Eijndhoven,¹³ D. Vannerom,¹⁵ J. van Santen,⁶² J. Vara,⁴³ J. Veitch-Michaelis,⁴⁰ M. Venugopal,³¹ M. Vereecken,³⁷ S. Verpoest,⁴⁴ D. Veske,⁴⁶ A. Vijai,¹⁹ C. Walck,⁵⁴ C. Weaver,²⁴ P. Weigel,¹⁵ A. Weindl,³¹ J. Weldert,⁵⁹ A. Y. Wen,¹⁴

C. Wendt,⁴⁰ J. Werthebach,²³ M. Weyrauch,³¹ N. Whitehorn,²⁴ C. H. Wiebusch,¹ N. Willey,²⁴ D. R. Williams,⁵⁷
 L. Witthaus,²³ A. Wolf,¹ M. Wolf,²⁷ G. Wrede,²⁶ X. W. Xu,⁷ J. P. Yanez,²⁵ E. Yildizci,⁴⁰ S. Yoshida,¹⁶ R. Young,³⁶ F. Yu,¹⁴
 S. Yu,²⁴ Z. Zhang,⁵⁵ P. Zhelmin,¹⁴ P. Zilberman,⁴⁰ and M. Zimmerman⁴⁰

(IceCube Collaboration)[§]

¹*III. Physikalisches Institut, RWTH Aachen University, D-52056 Aachen, Germany*

²*Department of Physics, University of Adelaide, Adelaide, 5005, Australia*

³*Department of Physics and Astronomy, University of Alaska Anchorage, 3211 Providence Dr., Anchorage, Alaska 99508, USA*

⁴*Department of Physics, University of Texas at Arlington, 502 Yates St., Science Hall Rm 108, Box 19059, Arlington, Texas 76019, USA*

⁵*CTSPS, Clark-Atlanta University, Atlanta, Georgia 30314, USA*

⁶*School of Physics and Center for Relativistic Astrophysics, Georgia Institute of Technology, Atlanta, Georgia 30332, USA*

⁷*Department of Physics, Southern University, Baton Rouge, Louisiana 70813, USA*

⁸*Department of Physics, University of California, Berkeley, California 94720, USA*

⁹*Lawrence Berkeley National Laboratory, Berkeley, California 94720, USA*

¹⁰*Institut für Physik, Humboldt-Universität zu Berlin, D-12489 Berlin, Germany*

¹¹*Fakultät für Physik & Astronomie, Ruhr-Universität Bochum, D-44780 Bochum, Germany*

¹²*Université Libre de Bruxelles, Science Faculty CP230, B-1050 Brussels, Belgium*

¹³*Vrije Universiteit Brussel (VUB), Dienst ELEM, B-1050 Brussels, Belgium*

¹⁴*Department of Physics and Laboratory for Particle Physics and Cosmology,*

Harvard University, Cambridge, Massachusetts 02138, USA

¹⁵*Department of Physics, Massachusetts Institute of Technology, Cambridge, Massachusetts 02139, USA*

¹⁶*Department of Physics and The International Center for Hadron Astrophysics, Chiba University, Chiba 263-8522, Japan*

¹⁷*Department of Physics, Loyola University Chicago, Chicago, Illinois 60660, USA*

¹⁸*Department of Physics and Astronomy, University of Canterbury, Private Bag 4800, Christchurch, New Zealand*

¹⁹*Department of Physics, University of Maryland, College Park, Maryland 20742, USA*

²⁰*Department of Astronomy, Ohio State University, Columbus, Ohio 43210, USA*

²¹*Department of Physics and Center for Cosmology and Astro-Particle Physics, Ohio State University, Columbus, Ohio 43210, USA*

²²*Niels Bohr Institute, University of Copenhagen, DK-2100 Copenhagen, Denmark*

²³*Department of Physics, TU Dortmund University, D-44221 Dortmund, Germany*

²⁴*Department of Physics and Astronomy, Michigan State University, East Lansing, Michigan 48824, USA*

²⁵*Department of Physics, University of Alberta, Edmonton, Alberta, Canada T6G 2E1*

²⁶*Erlangen Centre for Astroparticle Physics, Friedrich-Alexander-Universität Erlangen-Nürnberg, D-91058 Erlangen, Germany*

²⁷*Physik-department, Technische Universität München, D-85748 Garching, Germany*

²⁸*Département de physique nucléaire et corpusculaire, Université de Genève, CH-1211 Genève, Switzerland*

²⁹*Department of Physics and Astronomy, University of Gent, B-9000 Gent, Belgium*

³⁰*Department of Physics and Astronomy, University of California, Irvine, California 92697, USA*

³¹*Karlsruhe Institute of Technology, Institute for Astroparticle Physics, D-76021 Karlsruhe, Germany*

³²*Karlsruhe Institute of Technology, Institute of Experimental Particle Physics, D-76021 Karlsruhe, Germany*

³³*Department of Physics, Engineering Physics, and Astronomy, Queen's University, Kingston, Ontario K7L 3N6, Canada*

³⁴*Department of Physics & Astronomy, University of Nevada, Las Vegas, Nevada, 89154, USA*

³⁵*Nevada Center for Astrophysics, University of Nevada, Las Vegas, Nevada 89154, USA*

³⁶*Department of Physics and Astronomy, University of Kansas, Lawrence, Kansas 66045, USA*

³⁷*Centre for Cosmology, Particle Physics and Phenomenology—CP3, Université catholique de Louvain, Louvain-la-Neuve, Belgium*

³⁸*Department of Physics, Mercer University, Macon, Georgia 31207-0001, USA*

³⁹*Department of Astronomy, University of Wisconsin—Madison, Madison, Wisconsin 53706, USA*

⁴⁰*Department of Physics and Wisconsin IceCube Particle Astrophysics Center,*

University of Wisconsin—Madison, Madison, Wisconsin 53706, USA

⁴¹*Institute of Physics, University of Mainz, Staudinger Weg 7, D-55099 Mainz, Germany*

⁴²*Department of Physics, Marquette University, Milwaukee, Wisconsin 53201, USA*

⁴³*Institut für Kernphysik, Westfälische Wilhelms-Universität Münster, D-48149 Münster, Germany*

⁴⁴*Bartol Research Institute and Department of Physics and Astronomy, University of Delaware, Newark, Delaware 19716, USA*

⁴⁵*Department of Physics, Yale University, New Haven, Connecticut 06520, USA*

⁴⁶*Columbia Astrophysics and Nevis Laboratories, Columbia University, New York, New York 10027, USA*


⁴⁷*Department of Physics, University of Oxford, Parks Road, Oxford OX1 3PU, United Kingdom*

⁴⁸*Dipartimento di Fisica e Astronomia Galileo Galilei, Università Degli Studi di Padova, 35122 Padova PD, Italy*

⁴⁹*Department of Physics, Drexel University, 3141 Chestnut Street, Philadelphia, Pennsylvania 19104, USA*

⁵⁰*Physics Department, South Dakota School of Mines and Technology, Rapid City, South Dakota 57701, USA*

⁵¹*Department of Physics, University of Wisconsin, River Falls, Wisconsin 54022, USA*

⁵²*Department of Physics and Astronomy, University of Rochester, Rochester, New York 14627, USA*⁵³*Department of Physics and Astronomy, University of Utah, Salt Lake City, Utah 84112, USA*⁵⁴*Oskar Klein Centre and Department of Physics, Stockholm University, SE-10691 Stockholm, Sweden*⁵⁵*Department of Physics and Astronomy, Stony Brook University, Stony Brook, New York 11794-3800, USA*⁵⁶*Department of Physics, Sungkyunkwan University, Suwon 16419, Korea*⁵⁷*Department of Physics and Astronomy, University of Alabama, Tuscaloosa, Alabama 35487, USA*⁵⁸*Department of Astronomy and Astrophysics, Pennsylvania State University, University Park, Pennsylvania 16802, USA*⁵⁹*Department of Physics, Pennsylvania State University, University Park, Pennsylvania 16802, USA*⁶⁰*Department of Physics and Astronomy, Uppsala University, Box 516, S-75120 Uppsala, Sweden*⁶¹*Department of Physics, University of Wuppertal, D-42119 Wuppertal, Germany*⁶²*Deutsches Elektronen-Synchrotron DESY, Platanenallee 6, 15738 Zeuthen, Germany* (Received 22 July 2023; revised 15 February 2024; accepted 29 February 2024; published 11 April 2024)

We report on a measurement of astrophysical tau neutrinos with 9.7 yr of IceCube data. Using convolutional neural networks trained on images derived from simulated events, seven candidate ν_τ events were found with visible energies ranging from roughly 20 TeV to 1 PeV and a median expected parent ν_τ energy of about 200 TeV. Considering backgrounds from astrophysical and atmospheric neutrinos, and muons from π^\pm/K^\pm decays in atmospheric air showers, we obtain a total estimated background of about 0.5 events, dominated by non- ν_τ astrophysical neutrinos. Thus, we rule out the absence of astrophysical ν_τ at the 5σ level. The measured astrophysical ν_τ flux is consistent with expectations based on previously published IceCube astrophysical neutrino flux measurements and neutrino oscillations.

DOI: [10.1103/PhysRevLett.132.151001](https://doi.org/10.1103/PhysRevLett.132.151001)

In 2013 IceCube discovered a flux of neutrinos of astrophysical origin [1–3]. The astrophysical neutrino (ν^{astro}) flux normalization and index γ carry information about neutrino sources and their environments [4–15]. Different ν^{astro} production mechanisms lead to different $\nu_e:\nu_\mu:\nu_\tau$ ratios at the sources but, after standard neutrino oscillations over astrophysical distances, detectable numbers of all three neutrino flavors are expected at Earth [16–24]. Previous measurements at lower energies, using neutrinos produced at accelerators and in the atmosphere (ν^{atm}), have detected ν_τ produced directly [25] and through neutrino oscillations [26–28]. At the much higher energies accessible to this analysis, ν_τ^{atm} are strongly suppressed relative to ν_τ^{astro} [29], while an unexpected level of presence of ν_τ^{astro} in the ν^{astro} flux could be an indication of new physics [30–43].

Previous analyses [44–47] by IceCube to detect ν_τ^{astro} included searches for double-cascade signatures, such as the distinctive “double bang” [16] in the full detector or “double pulse” (DP) waveforms in one or two individual photosensors. The DP signature is produced by the distinct arrival times of light signals at one or more photosensors from the ν_τ interaction and τ decay vertices. IceCube previously observed two candidate ν_τ^{astro} , ruling out the null hypothesis of no ν_τ^{astro} at 2.8σ [46]. The analysis presented in this Letter reports on the low-background, high-significance detection of seven ν_τ^{astro} candidate events through the use of convolutional neural networks (CNNs).

IceCube [48] is a neutrino observatory with 5160 digital optical modules (DOMs) on 86 strings [48,49] in a cubic kilometer of ice at the South Pole. Charged particles

produced in neutrino interactions emit Cherenkov light [50] while propagating through the ice; photomultiplier tubes in the DOMs convert this light into electrical pulses that are digitized *in situ*. Light is deposited in the detector in several distinct patterns: long tracks, single cascades, and double cascades. Tracks are produced by muons from, e.g., ν_μ charged-current (CC) interactions, and can start or end inside, or pass through, the detector. Single cascades arise from electromagnetic and/or hadronic particle showers produced by deep inelastic neutrino-nucleon interactions in or near the detector, or by $\bar{\nu}_e$ via the Glashow resonance [51,52]. Double cascades are formed by high-energy $\nu_{\tau,\text{CC}}$ interactions in or near the detector that produce a hadronic shower and a τ lepton at the interaction vertex, followed by a second electromagnetic or hadronic shower at the τ decay vertex ($\text{BR}[\tau \rightarrow (e, h)] \simeq 83\%$). With a decay length of ~ 50 m/PeV, the τ can travel a macroscopic distance in the ice. For ν_τ energies satisfying $E_{\nu_\tau} \gtrsim 1$ PeV and favorable geometric containment, the double-bang signature can be created, with two energetic and well-separated cascades. Such events are intrinsically rare. In contrast, for lower E_{ν_τ} between roughly 50 TeV–1 PeV, the ν_τ flux is expected to be higher but in CC interactions the two cascades are closer together. Two cascades as close as about 10 m can produce distinctive patterns correlated across multiple DOMs and strings as the light from each cascade passes by, as well as DP waveforms in one or more DOMs.

We analyzed 9.7 yr of IceCube data from 2011–2020, triggering on approximately 10^{12} downward-going cosmic-

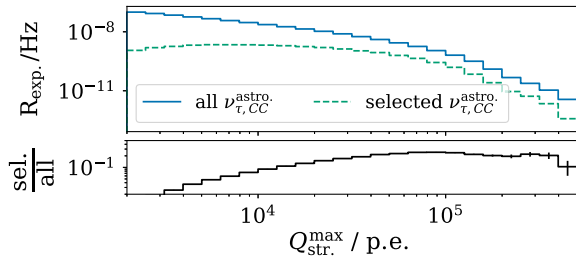


FIG. 1. Top: Simulated rate of $\nu_{\tau}^{\text{astro}}$ CC events binned by the number of p. e. detected by DOMs on the most illuminated string in the event, $Q_{\text{str}}^{\text{max}}$, before any selection criteria (solid) and after the CNN-based criteria (dashed) described in the text. (Downward-going cosmic-ray muons trigger the detector at about 3 kHz, are effectively removed by our selection criteria, and are not shown on the plot; other backgrounds are similarly heavily reduced and also not shown.) Bottom: Ratio of rates (selected or all), showing that signal efficiency grows above about 2000 p.e. The IceCube “GlobalFit” ν^{astro} flux [53] is assumed. (Error bars are statistical only.)

ray muons, $10^6 \nu^{\text{atm}}$, and $10^4 \nu^{\text{astro}}$ [53–56]. We required that the DOMs on the most illuminated string collected at least 2000 photoelectrons (p. e.) (see Fig. 1) and at least 10 p. e. in the two next-highest-charge, nearest-neighbor strings. Signal events will appear more like cascades than tracks in IceCube, so we also selected events whose morphology was better described by the cascade hypothesis. Aside from 0.6% (22 live days) of the data sample used to confirm agreement between data and simulation (data that were subsequently excluded from our analysis and which contained no signal-like events), we performed a “blind” analysis that only used simulated data to devise all selection criteria and analysis methodologies. After application of these initial selection criteria, there was roughly 300 times more background than signal. The expected number of p. e. on the most illuminated string for $\nu_{\tau}^{\text{astro}}$ CC events after application of these criteria, and additional CNN criteria described below, is shown in Fig. 1.

We then created 2D images of DOM number (corresponding to depth) vs time in 3.3 ns bins, with each pixel’s brightness proportional to the digitized waveform amplitude in that time bin. Images were created for the 180 DOMs on the most illuminated string and its two nearest and highest-illuminated neighbors, providing three images per event. The image for the highest-charge string on a candidate signal event is shown in Fig. 2 (left). The three images were then processed by CNNs, trained to distinguish images produced by simulated signal and background events and based on VGG16 [57], with a total of $\mathcal{O}(100 \text{ M})$ trainable parameters for the high-dimensional signal parameter space. Three separate CNNs were used to distinguish the ν_{τ} signal from remaining backgrounds produced by (i) single cascade neutrino interactions such as $\nu_{e,\mu,\tau}$ neutral current (NC) and ν_e CC, (ii) downward-going muons (μ_{\downarrow}), and (iii) both ν_{μ} interactions producing muon tracks and μ_{\downarrow} ; the associated

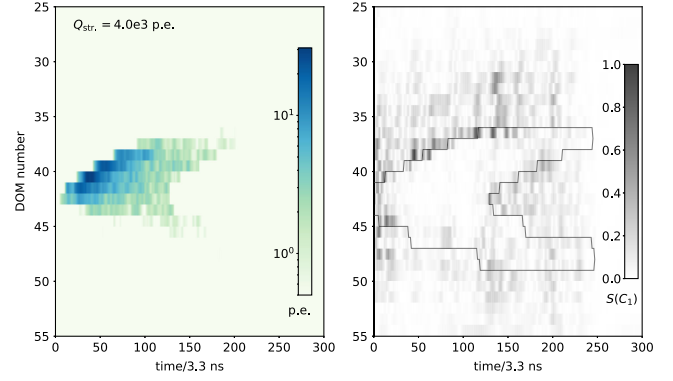


FIG. 2. Candidate $\nu_{\tau}^{\text{astro}}$ detected in September 2015. The left plot shows the DOM number (proportional to depth) versus the time of the digitized PMT signal in 3.3 ns bins for the highest-charge string, with the scale giving the signal amplitude in p.e. in each time bin. The total p.e. detected on the string, Q_{str} , is shown. The right plot shows $S(C_1)$, that string’s saliency map for C_1 , with darker regions indicating where the C_1 score is more sensitive to a changing light level (see text). (The Supplemental Material [59] shows three-string views and signed saliencies for all seven $\nu_{\tau}^{\text{astro}}$ candidates).

CNN scores are denoted C_1 , C_2 , and C_3 , respectively, with ranges $[0,1]$. Figure 2 (right) shows $S(C_1)$, the saliency [58] for C_1 , here defined as the magnitude of the gradient of the CNN score (scaled to $[0,1]$) of C_1 with respect to the signal amplitude at each pixel. For reference, the contour (solid line) shows where the detected light falls to zero, and is essentially an outline of the plot on the left. (Points outside the contour are variously acausally early, very late, or at distances that are many absorption lengths from the event vertices.) Large $S(C_1)$ values indicate where and when changes in light level most effectively change C_1 . Small $S(C_1)$ values appear in highly illuminated regions and in regions with no light. Bright regions contribute to C_1 , but C_1 is not as sensitive there to changes in light level as at the leading and trailing edge envelopes of the light from the event, which are roughly coincident with the contour. The saliency thus shows that C_1 is sensitive to the overall shape of emitted light in the detector.

The scores were calculated for each event, and a signal-to-noise ratio of ~ 14 was obtained by requiring events to have high scores ($C_1 \geq 0.99$, $C_2 \geq 0.98$ and $C_3 \geq 0.85$). The dominant backgrounds come from other ν^{astro} flavors and ν^{atm} . The expected energy spectra for signal and the dominant backgrounds, after application of initial and then final selection criteria (including the high CNN scores), are shown in Fig. 3.

A subdominant “edge event” background was observed from simulated cosmic-ray muons that deposited most of their Cherenkov light on a single string on the outer edge of the detector. We required $C_3 > 0.95$ for edge events, reducing this background by about an order of magnitude at an estimated 15% signal loss. Table I lists the expected

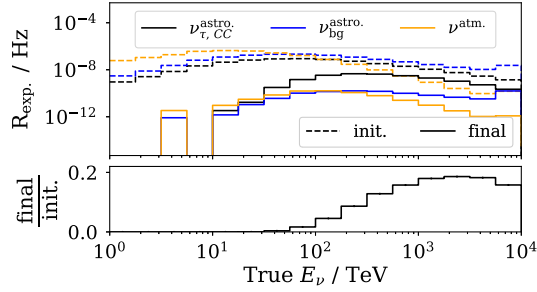


FIG. 3. Top: Expected rate vs energy of $\nu_{\tau}^{\text{astro}}$ CC events, astrophysical and atmospheric neutrino backgrounds with initial selection criteria applied (dashed) and with final selection criteria then also applied (solid); for $\nu_{\tau}^{\text{astro}}$ the IceCube GlobalFit flux [53] was assumed. Bottom: Ratio of $\nu_{\tau}^{\text{astro}}$ CC rates after final and initial selection criteria. (Statistical error bars are too small to be visible. Although not shown in the plot, the backgrounds were simulated up to $E_{\nu} = 100$ PeV).

number of events, after application of the initial and final sets of selection criteria, assuming the best-fit parameters from two IceCube flux measurements.

The largest backgrounds are due to other astrophysical neutrino interactions, and conventional and prompt atmospheric neutrinos, followed by muons from π^{\pm}/K^{\pm} decays in cosmic-ray air showers. The backgrounds listed in Table I were estimated using simulation packages for astrophysical neutrinos [71], muons from cosmic-ray air showers [79,80] (with cosmic-ray primary flux given by [81] and hadronic interaction model by [82]), conventional atmospheric neutrino flux from π^{\pm}/K^{\pm} decays [72] following our published ν^{atm} flux measurements above $E_{\nu} \sim 50$ TeV [73–75], and prompt atmospheric neutrino flux [56,76–78] postulated to arise from the decays of charm or heavier mesons produced in air showers and modeled following Ref. [76]. Electromagnetic (EM) and hadronic showers below 1 PeV were simulated based on the parametrizations of the mean longitudinal and lateral profiles in Ref. [83] and included fluctuations in the energy of the hadronic component. Above 1 PeV the LPM effect [84–86] is used for EM showers. (Our treatment of possible prompt atmospheric muons is described in the Supplemental Material [59].) The total νN deep inelastic scattering cross section is from [87].

TABLE I. Expected number of events after initial and final set of selection criteria (including all corrections described in the text) for signal ($\nu_{\tau, \text{CC}}^{\text{astro}}$) and backgrounds, assuming IceCube’s flux from Refs. [53] and (in parentheses) [56]. About 85% of the estimated contribution from $\nu_{\text{prompt}}^{\text{atm}}$ is from ν_{τ} . Signal and astrophysical background levels vary with the flux. The simulation did not include the self-veto effect [70] that would reduce the conventional (conv.) and prompt ν^{atm} backgrounds. References to associated simulation packages are given; see text for details. Errors are statistical only, arising from finite simulation samples.

	$\nu_{\tau, \text{CC}}^{\text{astro}}$ [71]	$\nu_{\text{other}}^{\text{astro}}$ [71]	$\nu_{\text{conv.}}^{\text{atm}}$ [72–75]	$\nu_{\text{prompt}}^{\text{atm}}$ [56,76–78]	$\mu_{\text{conv.}}^{\text{atm}}$ [79–82]	All background
Initial	160 ± 0.2 (190 ± 0.3)	400 ± 0.7 (490 ± 0.8)	580 ± 7	72 ± 0.1	8400 ± 110	9450 ± 110 (9540 ± 110)
Final	6.4 ± 0.02 (4.0 ± 0.02)	0.3 ± 0.02 (0.2 ± 0.01)	0.1 ± 0.008	0.1 ± 0.001	0.01 ± 0.008	0.5 ± 0.02 (0.4 ± 0.02)

Additional potential background from muon deep inelastic scattering (μ DIS), given by $\mu + X \rightarrow \nu_{\mu} + X'$, where the light from the incoming μ followed by the light from the hadronic cascade could mimic the ν_{τ} signature, is estimated from the predicted atmospheric ν_{μ} CC background. At energies above roughly 100 TeV, we expect comparable numbers of atmospheric ν_{μ} and μ [70], but the μ energies will be diminished as they pass through the ice to the detector, decreasing their ability to mimic the ν_{τ} signature. We conservatively doubled the estimated background from atmospheric ν_{μ} CC interactions, from 0.005 to 0.01, to account for the potential background.

We also estimated the background expected from charmed hadrons produced in energetic ν_e CC and ν NC interactions. This background component had not initially been considered in designing the analysis. After unblinding, we became aware of recent results [88] that indicate that the strange sea in the nucleon is not as suppressed as had been previously believed, so that charm production would thereby be somewhat enhanced compared to our original estimate. Using a simulated neutrino dataset based on the HERAPDF1.5 [89] parton distribution functions (PDFs), and applying a modest correction to reflect more modern PDFs [88,90–93], the estimated background from ν^{astro} increases by 23% relative to the simulations excluding these interactions. The theoretical uncertainty from the PDFs at the 100 TeV scale is roughly 3%, so the increase corresponds to only about $(15 \pm 0.5)\%$ (0.08 ± 0.002 events) of the total background estimation. We included this additional background directly to maintain our blindness protocol that disallowed retraining the CNNs to reject charm background. Uncertainties in the cross section for the interaction of charmed mesons and baryons with ordinary matter had a negligible impact. Backgrounds from on-shell W production [94] from high-energy ν_e/ν_{μ} interactions, top-quark decay, and Glashow resonance interactions [95] can produce energetic ν_{τ} or τ , but are collectively estimated to contribute roughly an order of magnitude fewer background events than other sources and were not included in our background estimate.

For the range of astrophysical neutrino fluxes measured by IceCube (denoted $\phi_{\text{astro}}^{\text{IC}}$), and for a 1 : 1 : 1 neutrino flavor ratio at the detector, we predicted a final sample of 4–8 ν_{τ}

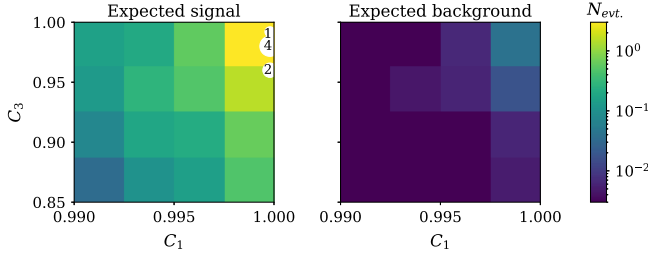


FIG. 4. Histogram of the C_3 vs C_1 CNN scores with all selection criteria applied. The color in each bin gives the expected number of signal (left) and background (right) events in that bin, assuming IceCube’s GlobalFit flux [53]. The approximate (C_1, C_3) values of the seven observed candidate ν_τ^{astro} are shown by white circles, with the number inside each circle indicating the number of candidate events there.

CC signal events. Similarly, the predicted total background varied for each $\phi_{\text{astro}}^{\text{IC}}$. Using IceCube’s previous measurements of the spectral index γ_{astro} , this relatively small number of events constrains the ν_{astro} flux normalization ϕ_{astro} . Data satisfying $C_2 > 0.98$ were placed in 4×4 bins in their C_1 and C_3 scores.

We calculated confidence intervals following Ref. [96] and using the test statistic defined as $\text{TS}(\lambda_\tau) = \ln L(\hat{\lambda}_\tau) - \ln L(\lambda_\tau)$, where $\lambda_\tau = \phi(\nu_\tau^{\text{astro}})/\phi_{\text{nom}}(\nu_\tau^{\text{astro}})$, the measured-to-nominal flux ratio. Here the nominal flux is one of the four IceCube measured values, and $\hat{\lambda}_\tau$ the value of λ_τ that maximizes the Poisson likelihood L across all 16 bins. Critical values were extracted at the desired confidence level using the TS distributions from a range of λ_τ values, each of which were simulated with 10^4 pseudo experiments. This procedure incorporated as nuisance parameters the systematic uncertainties in the estimated fluxes for each background component (prior width of 30% for ν^{atm} and ν^{astro} ; 50% for cosmic-ray muons), the detection efficiency of the DOMs (10%), and the optical scattering properties of the ice (5%). Since many of these parameters are degenerate in their effect on the analysis observables, and we expected fewer signal events than nuisance parameters, we estimated their impact by incorporating randomized versions of the parameters for each of the pseudo experiments used to calculate the critical value of our TS. This procedure increased the critical values relative to their values in the absence of the systematic uncertainties, widening the extracted confidence intervals.

Seven events remained after applying the final set of selection criteria to the data, consistent with expectation. Figure 4 shows the final expected signal and background, assuming IceCube’s GlobalFit flux, as a function of C_3 vs C_1 . Five of the candidate ν_τ events are in the upper right bin and two are in the bin just below it. Three of the seven events were seen in previous IceCube analyses [1,46,47,97], and one of these three had previously been identified [46,47] as a candidate ν_τ^{astro} . For each candidate event we

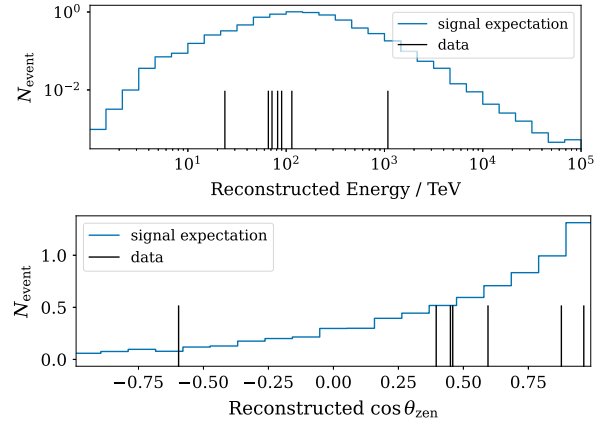


FIG. 5. Reconstructed visible energies (top) and $\cos \theta_{\text{zen}}$ (bottom) for simulated ν_τ^{CC} (solid histogram) and seven candidate events (vertical lines) for the flux in Ref. [53]. The upward-going event with $\cos \theta_{\text{zen}} \simeq -0.6$ had a reconstructed energy of ~ 90 TeV.

evaluated the “tauness” as $P_\tau(i) = n_s(i)/[n_s(i) + n_b(i)]$, where n_s and n_b are the expected signal and background in bin i (see Fig. 4). P_τ ranges from 0.90–0.92 for two of the candidate ν_τ , and 0.94–0.95 for the other five, depending on the assumed $\phi_{\text{astro}}^{\text{IC}}$. For IceCube’s GlobalFit flux we predict a total background of 0.5 ± 0.02 events (see Table I); using the distribution of the seven observed events and expected backgrounds in the 16 bins in Fig. 4, we exclude the null hypothesis of no ν_τ^{astro} at a (single-sided) significance of 5.1σ . Under the other three flux assumptions [54–56], the significances are 5.2σ , 5.2σ , and 5.5σ , respectively. The best-fit ν_τ flux normalizations are all within the 68% frequentist confidence intervals of the four IceCube fluxes.

We performed multiple checks on the candidate events to ensure they were consistent with expectation. For simplicity and to avoid introducing additional systematic uncertainties, the analysis did not employ a tailored ν_τ^{astro} reconstruction. However, as a post-unblinding check we used a reconstruction for single-cascade events [98] to estimate the energies and directions (Fig. 5) and vertex positions (see Supplemental Material [59]). The median expected E_{ν_τ} was roughly 200 TeV (for the flux in Ref. [53]). The dominant up-down asymmetry is due to Earth absorption and consistent with expectation. Other polar angle effects such as higher vertical vs horizontal DOM density and ν_τ regeneration [99] are also included. (Simulations predict that for $E_\tau \lesssim 0.5$ PeV, the selected events are biased toward higher average τ decay lengths $\langle L_\tau \rangle$; e.g., for $E_\tau \sim 100$ TeV, $\langle L_\tau \rangle \sim 10$ m). The events were more clustered in depth than expected but were consistent with a statistical fluctuation, as discussed in the Supplemental Material [59]. We observed no significant coincident activity in the IceTop cosmic-ray air-shower surface array for any of the events.

We tested the robustness of the CNNs to hypothetical improperly modeled uncertainties by evaluating their

susceptibility to correlated and uncorrelated variations of the raw data underlying the images. We found that the probability of background-to-signal migration was $< (2 \pm 0.2) \times 10^{-5}$ and of signal-to-background migration $< (3 \pm 0.8) \times 10^{-3}$. We also employed targeted tests to estimate the CNNs' robustness against less likely changes in the underlying raw data, including adversarial attacks [100] against candidate signal and simulated background events. We found that events only migrated in response to changes outside our uncertainty envelope. These tests are described in the Supplemental Material [59]. We conclude that the CNNs are robust against detector systematic effects that could present as either uncorrelated or correlated changes in light levels in one or more DOMs, or entire strings, in the detector.

Energetic astrophysical sources, in conjunction with neutrino oscillations over cosmic baselines, provide the only known way to produce large numbers of ν_τ energetic enough to create the observed event morphologies. The result presented in this Letter demonstrates that astrophysical ν_τ consistent with this hypothesis are present in the IceCube data and provides powerful confirmation of the earlier IceCube discovery of astrophysical neutrinos [2,3,101].

The IceCube Collaboration acknowledges the significant contributions to this manuscript from the Pennsylvania State University. USA: U.S. National Science Foundation-Office of Polar Programs, U.S. National Science Foundation-Physics Division, U.S. National Science Foundation-EPSCoR, U.S. National Science Foundation-Major Research Instrumentation Program, Deep Learning for Statistics, Astrophysics, Geoscience, Engineering, Meteorology and Atmospheric Science, Physical Sciences and Psychology (DL-SAGEMAPP) at the Institute for Computational and Data Sciences (ICDS) at the Pennsylvania State University, Wisconsin Alumni Research Foundation, Center for High Throughput Computing (CHTC) at the University of Wisconsin-Madison, Open Science Grid (OSG), Advanced Cyberinfrastructure Coordination Ecosystem: Services & Support (ACCESS), Frontera computing project at the Texas Advanced Computing Center, U.S. Department of Energy-National Energy Research Scientific Computing Center, Particle astrophysics research computing center at the University of Maryland, Institute for Cyber-Enabled Research at Michigan State University, and Astroparticle physics computational facility at Marquette University; Belgium: Funds for Scientific Research (FRS-FNRS and FWO), FWO Odysseus and Big Science programmes, and Belgian Federal Science Policy Office (Belspo); Germany: Bundesministerium für Bildung und Forschung (BMBF), Deutsche Forschungsgemeinschaft (DFG), Helmholtz Alliance for Astroparticle Physics (HAP), Initiative and Networking Fund of the Helmholtz Association, Deutsches Elektronen Synchrotron (DESY), and High Performance

Computing cluster of the RWTH Aachen; Sweden: Swedish Research Council, Swedish Polar Research Secretariat, Swedish National Infrastructure for Computing (SNIC), and Knut and Alice Wallenberg Foundation; European Union: EGI Advanced Computing for research; Australia: Australian Research Council; Canada: Natural Sciences and Engineering Research Council of Canada, Calcul Québec, Compute Ontario, Canada Foundation for Innovation, WestGrid, and Compute Canada; Denmark: Villum Fonden, Carlsberg Foundation, and European Commission; New Zealand: Marsden Fund; Japan: Japan Society for Promotion of Science (JSPS) and Institute for Global Prominent Research (IGPR) of Chiba University; Korea: National Research Foundation of Korea (NRF); Switzerland: Swiss National Science Foundation (SNSF); United Kingdom: Department of Physics, University of Oxford.

* Also at Institute of Physics, Sachivalaya Marg, Sainik School Post, Bhubaneswar 751005, India.

† Also at Department of Space, Earth and Environment, Chalmers University of Technology, 412 96 Gothenburg, Sweden.

‡ Also at Earthquake Research Institute, University of Tokyo, Bunkyo, Tokyo 113-0032, Japan.

§ analysis@icecube.wisc.edu

- [1] M. G. Aartsen *et al.* (IceCube Collaboration), *Phys. Rev. Lett.* **111**, 021103 (2013).
- [2] M. G. Aartsen *et al.* (IceCube Collaboration), *Science* **342**, 1242856 (2013).
- [3] M. G. Aartsen *et al.* (IceCube Collaboration), *Phys. Rev. Lett.* **113**, 101101 (2014).
- [4] E. Fermi, *Phys. Rev.* **75**, 1169 (1949).
- [5] A. R. Bell, *Mon. Not. R. Astron. Soc.* **182**, 147 (1978).
- [6] T. K. Gaisser, *Cosmic Rays and Particle Physics* (Cambridge University Press, Cambridge, England, 1990).
- [7] R. J. Protheroe and D. Kazanas, *Astrophys. J.* **265**, 620 (1983).
- [8] D. Kazanas and D. C. Ellison, *Astrophys. J.* **304**, 178 (1986).
- [9] M. Sikora, J. G. Kirk, M. C. Begelman, and P. Schneider, *Astrophys. J. Lett.* **320**, L81 (1987).
- [10] F. W. Stecker, C. Done, M. H. Salamon, and P. Sommers, *Phys. Rev. Lett.* **66**, 2697 (1991).
- [11] F. W. Stecker, C. Done, M. H. Salamon, and P. Sommers, *Phys. Rev. Lett.* **69**, 2738(E) (1992).
- [12] K. Mannheim and P. L. Biermann, *Astron. Astrophys.* **253**, L21 (1992).
- [13] J. Matthews, A. Bell, and K. Blundell, *New Astron. Rev.* **89**, 101543 (2020).
- [14] W. Winter, *Phys. Rev. D* **88**, 083007 (2013).
- [15] K. Murase, M. Ahlers, and B. C. Lacki, *Phys. Rev. D* **88**, 121301(R) (2013).
- [16] J. G. Learned and S. Pakvasa, *Astropart. Phys.* **3**, 267 (1995).
- [17] H. Athar, C. S. Kim, and J. Lee, *Mod. Phys. Lett. A* **21**, 1049 (2006).

- [18] T. Kashti and E. Waxman, *Phys. Rev. Lett.* **95**, 181101 (2005).
- [19] S. R. Klein, R. E. Mikkelsen, and J. Becker Tjus, *Astrophys. J.* **779**, 106 (2013).
- [20] P. Lipari, M. Lusignoli, and D. Meloni, *Phys. Rev. D* **75**, 123005 (2007).
- [21] M. Bustamante, J. F. Beacom, and W. Winter, *Phys. Rev. Lett.* **115**, 161302 (2015).
- [22] A. Esmaili and Y. Farzan, *Nucl. Phys.* **B821**, 197 (2009).
- [23] I. Esteban, M. C. Gonzalez-Garcia, A. Hernandez-Cabezudo, M. Maltoni, and T. Schwetz, *J. High Energy Phys.* **01** (2019) 106.
- [24] NuFIT 4.1, www.nu-fit.org (2019).
- [25] K. Kodama *et al.* (DONuT Collaboration), *Phys. Rev. D* **78**, 052002 (2008).
- [26] N. Agafonova *et al.* (OPERA Collaboration), *Phys. Rev. D* **100**, 051301 (2019).
- [27] Z. Li *et al.* (Super-Kamiokande Collaboration), *Phys. Rev. D* **98**, 052006 (2018).
- [28] M. G. Aartsen *et al.* (IceCube Collaboration), *Phys. Rev. D* **99**, 032007 (2019).
- [29] A. Bhattacharya, R. Enberg, Y. S. Jeong, C. S. Kim, M. H. Reno, I. Sarcevic, and A. Stasto, *J. High Energy Phys.* **11** (2016) 167.
- [30] C. A. Argüelles, T. Katori, and J. Salvado, *Phys. Rev. Lett.* **115**, 161303 (2015).
- [31] G. Pagliaroli, A. Palladino, F. L. Villante, and F. Vissani, *Phys. Rev. D* **92**, 113008 (2015).
- [32] I. M. Shoemaker and K. Murase, *Phys. Rev. D* **93**, 085004 (2016).
- [33] V. Brdar, J. Kopp, and X.-P. Wang, *J. Cosmol. Astropart. Phys.* **01** (2017) 026.
- [34] M. Bustamante, J. F. Beacom, and K. Murase, *Phys. Rev. D* **95**, 063013 (2017).
- [35] N. Klop and S. Ando, *Phys. Rev. D* **97**, 063006 (2018).
- [36] R. W. Rasmussen, L. Lechner, M. Ackermann, M. Kowalski, and W. Winter, *Phys. Rev. D* **96**, 083018 (2017).
- [37] M. Bustamante and S. K. Agarwalla, *Phys. Rev. Lett.* **122**, 061103 (2019).
- [38] P. B. Denton and I. Tamborra, *Phys. Rev. Lett.* **121**, 121802 (2018).
- [39] Y. Farzan and S. Palomares-Ruiz, *Phys. Rev. D* **99**, 051702 (R) (2019).
- [40] R. Abbasi *et al.* (IceCube Collaboration), *Nat. Phys.* **18**, 1287 (2022).
- [41] A. Abdullahi and P. B. Denton, *Phys. Rev. D* **102**, 023018 (2020).
- [42] R. M. Abraham *et al.*, *J. Phys. G* **49**, 110501 (2022).
- [43] M. Ackermann *et al.*, *J. High Energy Astrophys.* **36**, 55 (2022).
- [44] R. Abbasi *et al.* (IceCube Collaboration), *Phys. Rev. D* **86**, 022005 (2012).
- [45] M. G. Aartsen *et al.* (IceCube Collaboration), *Phys. Rev. D* **93**, 022001 (2016).
- [46] R. Abbasi *et al.* (IceCube Collaboration), *Eur. Phys. J. C* **82**, 1031 (2022).
- [47] M. Meier and J. Soedingrekso (IceCube Collaboration), *Proc. Sci., ICRC2019* (2020) 960.
- [48] M. G. Aartsen *et al.* (IceCube Collaboration), *J. Instrum.* **12**, P03012 (2017).
- [49] R. Abbasi *et al.* (IceCube Collaboration), *Astropart. Phys.* **35**, 615 (2012).
- [50] P. A. Cherenkov, *Dokl. Akad. Nauk SSSR* **2**, 451 (1934).
- [51] S. L. Glashow, *Phys. Rev.* **118**, 1 (1960).
- [52] M. G. Aartsen *et al.* (IceCube Collaboration), *Nature (London)* **591**, 220 (2021); **592**, E11 (2021).
- [53] M. G. Aartsen *et al.* (IceCube Collaboration), *Astrophys. J.* **809**, 98 (2015).
- [54] R. Abbasi *et al.* (IceCube Collaboration), *Astrophys. J.* **928**, 50 (2022).
- [55] M. G. Aartsen *et al.* (IceCube Collaboration), *Phys. Rev. D* **99**, 032004 (2019).
- [56] R. Abbasi *et al.* (IceCube Collaboration), *Phys. Rev. D* **104**, 022002 (2021).
- [57] K. Simonyan and A. Zisserman, [arXiv:1409.1556](https://arxiv.org/abs/1409.1556).
- [58] K. Simonyan, A. Vedaldi, and A. Zisserman, [arXiv:1312.6034](https://arxiv.org/abs/1312.6034).
- [59] See Supplemental Material at <http://link.aps.org/supplemental/10.1103/PhysRevLett.132.151001>, which includes Refs. [60–69] for additional event displays, a more detailed discussion of backgrounds, and data-driven studies of the CNN performance.
- [60] A. G. Bogdanov, R. P. Kokoulin, Y. F. Novoseltsev, R. V. Novoseltseva, V. B. Petkov, and A. A. Petrukhin, *Astropart. Phys.* **36**, 224 (2012).
- [61] D. Chirkin (IceCube Collaboration), in *33rd International Cosmic Ray Conference* (Brazilian Journal of Physics, Rio de Janeiro, Brazil, 2013), p. 0580.
- [62] J. Ranft, *Phys. Rev. D* **51**, 64 (1995).
- [63] M. G. Aartsen *et al.* (IceCube Collaboration), *Nucl. Instrum. Methods Phys. Res., Sect. A* **711**, 73 (2013).
- [64] M. G. Aartsen *et al.* (IceCube Collaboration), *Astropart. Phys.* **78**, 1 (2016).
- [65] R. Abbasi *et al.* (IceCube Collaboration), *Comput. Phys. Commun.* **266**, 108018 (2021).
- [66] A. Kolmogorov, *G. Ist. Ital. Attuari* **4**, 83 (1933).
- [67] N. Kuiper, *Nederl Akad Wetensch Proc Ser A.* **63**, 38 (1960).
- [68] N. Y. Agafonova, M. Aglietta, P. Antonioli, V. V. Ashikhmin, G. Bari *et al.* (LVD Collaboration), *Phys. Rev. D* **100**, 062002 (2019).
- [69] D. Chirkin and M. Rongen, *Proc. Sci., ICRC2019* (2020) 854.
- [70] S. Schonert, T. K. Gaisser, E. Resconi, and O. Schulz, *Phys. Rev. D* **79**, 043009 (2009).
- [71] A. Gazizov and M. P. Kowalski, *Comput. Phys. Commun.* **172**, 203 (2005).
- [72] M. Honda, T. Kajita, K. Kasahara, S. Midorikawa, and T. Sanuki, *Phys. Rev. D* **75**, 043006 (2007).
- [73] R. Abbasi *et al.* (IceCube Collaboration), *Phys. Rev. D* **83**, 012001 (2011).
- [74] M. G. Aartsen *et al.* (IceCube Collaboration), *Phys. Rev. Lett.* **110**, 151105 (2013).
- [75] M. G. Aartsen *et al.* (IceCube Collaboration), *Phys. Rev. D* **91**, 122004 (2015).
- [76] A. Bhattacharya *et al.*, *J. High Energy Phys.* **06** (2015) 110.
- [77] M. V. Garzelli, S. Moch, and G. Sigl, *J. High Energy Phys.* **10** (2015) 115.

- [78] R. Gauld, J. Rojo, L. Rottoli, S. Sarkar, and J. Talbert, *J. High Energy Phys.* **02** (2016) 130.
- [79] D. Heck, J. Knapp, J.N. Capdevielle, G. Schatz, and T. Thouw, Report No. FZKA-6019, Universität Karlsruhe, Karlsruhe, Germany, 1998.
- [80] J. van Santen, Ph.D. thesis, University of Wisconsin-Madison, 2014.
- [81] T. K. Gaisser, *Astropart. Phys.* **35**, 801 (2012).
- [82] E. J. Ahn, R. Engel, T. K. Gaisser, P. Lipari, and T. Stanev, *Phys. Rev. D* **80**, 094003 (2009).
- [83] L. Radel and C. Wiebusch, *Astropart. Phys.* **44**, 102 (2013).
- [84] L. D. Landau and I. Pomeranchuk, Dokl. Akad. Nauk Ser. Fiz. **92**, 735 (1953).
- [85] L. D. Landau and I. Pomeranchuk, Dokl. Akad. Nauk Ser. Fiz. **92**, 535 (1953).
- [86] A. B. Migdal, *Phys. Rev.* **103**, 1811 (1956).
- [87] A. Cooper-Sarkar, P. Mertsch, and S. Sarkar, *J. High Energy Phys.* **08** (2011) 042.
- [88] G. Aad *et al.* (ATLAS Collaboration), *Eur. Phys. J. C* **82**, 438 (2022).
- [89] V. Radescu (H1, ZEUS Collaborations), *Proc. Sci., ICHEP2010* (2010) 168.
- [90] T.-J. Hou *et al.*, *Phys. Rev. D* **103**, 014013 (2021).
- [91] S. Bailey, T. Cridge, L. A. Harland-Lang, A. D. Martin, and R. S. Thorne, *Eur. Phys. J. C* **81**, 341 (2021).
- [92] F. Faura, S. Iranipour, E. R. Nocera, J. Rojo, and M. Ubiali, *Eur. Phys. J. C* **80**, 1168 (2020).
- [93] M. Aaboud *et al.* (ATLAS Collaboration), *Eur. Phys. J. C* **77**, 367 (2017).
- [94] B. Zhou and J. F. Beacom, *Phys. Rev. D* **101**, 036010 (2020).
- [95] A. G. Soto, P. Zhelmin, I. Safa, and C. A. Argüelles, *Phys. Rev. Lett.* **128**, 171101 (2022).
- [96] G. J. Feldman and R. D. Cousins, *Phys. Rev. D* **57**, 3873 (1998).
- [97] L. Lu (IceCube Collaboration), *Proc. Sci., ICRC2017* (2018) 1002.
- [98] M. Huenefeld *et al.* (IceCube Collaboration), *Proc. Sci., ICRC2021* (2021) 1065.
- [99] F. Halzen and D. Saltzberg, *Phys. Rev. Lett.* **81**, 4305 (1998).
- [100] S.-M. Moosavi-Dezfooli, A. Fawzi, and P. Frossard, in *Proceedings of the IEEE Conference on Computer Vision and Pattern Recognition* (IEEE, Las Vegas, Nevada, 2016), pp. 2574–2582.
- [101] M. G. Aartsen *et al.* (IceCube Collaboration), *Phys. Rev. Lett.* **111**, 021103 (2013).